

## Support Information

### **The role of Mott-Schottky heterojunctions in PtCo- Cu<sub>2</sub>ZnGeS<sub>4</sub> as counter electrodes in dye-sensitized solar cells**

Shoushuang Huang<sup>a</sup>, Qingquan He<sup>a</sup>, Jiantao Zai<sup>a,\*</sup>, Min Wang<sup>a</sup>, Xiaomin Li<sup>a</sup>, Bo Li<sup>a</sup>,  
Xuefeng Qian<sup>a,\*</sup>

[a] S. S. Huang,<sup>[+]</sup> Q. Q. He,<sup>[+]</sup> Dr. J. T. Zai, Prof. X. F. Qian

Shanghai Electrochemical Energy Devices Research Center, School of Chemistry and  
Chemical Engineering and State Key Laboratory of Metal Matrix Composites,  
Shanghai Jiao Tong University, Shanghai, 200240, P. R. China.

E-mail: xfqian@sjtu.edu.cn; zaijiantao@sjtu.edu.cn

[+] These authors contributed equally to this work.

## Experimental details:

### Chemical:

Copper (II) acetylacetonate ( $\text{Cu}(\text{acac})_2$ ; >99.99%), Zinc (II) acetylacetonate ( $\text{Zn}(\text{acac})_2$ ; >99.99%), Germanium (IV) chloride ( $\text{GeCl}_4$ ; >99.99%), and trioctylphosphine oxide Trioctylphosphine oxide (TOPO, 99%) were purchased from alfa Aesar; Oleylamine (OLAm, 70% tech) were purchased from Aldrich and 1-dodecanethiol (1-DDT, 98%), tert-Dodecanethiol (t-DDT) were purchased from TCI. All chemicals were used as received without any further purification.

### Synthesis of wurtstanite-type CZGS nanocrystals (NCs):

In a typical synthesis, 1 mmol copper (II)  $\text{Cu}(\text{acac})_2$ , 0.5 mmol  $\text{Zn}(\text{acac})_2$ , 0.5 mmol  $\text{GeCl}_4$ , and 1.5 mmol trioctylphosphine oxide were mixed with 10 mL of OLAm in a three-neck round bottom flask and evacuated at 100 °C for 30 min to eliminate adventitious water and dissolved oxygen. The solution was then heated to 140 °C under a nitrogen atmosphere and a mixture of 1.5 mmol of 1-dodecanethiol (1-DDT) and 10.0 mmol of tert-dodecyl mercaptan (t-DDT) was quickly injected into the flask. The mixture was subsequently heated to 280 °C and maintain at this temperature for 240 min to allow the growth of CZGS nanocrystals. Finally, the products were precipitated by ethanol and redispersed in organic solvent for further use.

### Synthesis of stannite CZGS nanocrystals:

In a three-neck flask,  $\text{Cu}(\text{acac})_2$  (0.261g, 1mmol),  $\text{Zn}(\text{acac})_2$  (0.132 g, 0.5 mmol),  $\text{GeCl}_4$  (0.107 g, 0.5 mmol) and TOPO (0.580 g, 1.5 mmol) were mixed with 10 mL of oleylamine. The contents of the flask were evacuated at room temperature for 30 minute to eliminate adventitious water and dissolved oxygen. The reaction mixture was then heated to 250°C ~ 260°C under argon flow and 1 mmol S power dissolved in 2 mL hot OAm was rapidly injected into the system at 140°C with continuous stirring. The nanocrystals were allowed to grow for 120 minutes to reach the desired size. After cooling to room temperature, the product was washed by precipitating with acetone, followed by centrifugation and subsequent resuspension in toluene or hexane. This was repeated a total of three times. The final product was centrifuged in either toluene or hexane to precipitate large agglomerates and the colloidal nanocrystals remained suspended in solution.

### **Synthesis of Pt<sub>3</sub>Co<sub>1</sub>-CZGS heterostructured NCs and Pt<sub>3</sub>Co<sub>1</sub> NCs:**

The as-obtained CZGS NCs were used as seeds to produce CZGS-Pt<sub>3</sub>Co<sub>1</sub> heterostructured NCs.<sup>1,2</sup> In a typical synthesis, 0.20 mL oleic acid, 0.20 mL OLAm, 40 mg 1, 2-hexadecanediol, and 10 mL phenyl ether were loaded into the reaction flask and kept at 120 °C for 30 min under a nitrogen flow. In parallel, 30 mg Pt(acac)<sub>2</sub> and 45 mg of Co(acac)<sub>2</sub> was mixed with a dispersion of the CZGS nanocrystals (120 mg) and heated at 80 °C for 30 min to promote the dissolution of metal salt. This CZGS suspension containing the Pt precursor was injected into the phenyl ether solution at 200 °C. After 10 min, the reaction was quenched in a water bath. The product was washed twice by precipitation in ethanol followed by centrifugation, and then separated twice by centrifugation. Pt<sub>3</sub>Co<sub>1</sub> NCs were synthesized according to the reported literature.<sup>3</sup>

### **Fabrication of DSSCs:**

The concentrated CZGS or CZGS-PtCo (~120 mg/mL) nanocrystal ink was coated on FTO glass by spin-coating to form a nanocrystal thin film. Subsequently, the films were annealed at 400 °C for 20 min under nitrogen atmosphere. For comparison, pyrolytic Pt CE was prepared by drop-casting 50 µL of H<sub>2</sub>PtCl<sub>6</sub> in ethanol (5 mM) on a 1.5 × 1.5 cm<sup>2</sup> FTO glass followed by sintering at 400 °C for 30 min. The commercial TiO<sub>2</sub> photoanodes (Ying kou Opvtech New Energy Co., Ltd) were first immersed into 40 mM TiCl<sub>4</sub> aqueous solution and kept in an oil bath at 70 °C for 30 min, and then annealed at 500 °C for 1 h. After being cooled to 80 °C, the TiO<sub>2</sub> photoanodes were immersed in a 0.5 mM ethanol solution of N719 dye (Solaronix SA, Switzerland) for 20 h. DSSCs were assembled by attaching dye-sensitized TiO<sub>2</sub> electrode with the CE with a 60-µm thick hot-melt film (Surlyn 1702; DuPont) as spacer and then sealed up by heating. The cell internal space was filled with electrolytes using a vacuum pump. The liquid electrolyte were prepared by dissolving 798.3 mg of 1-butyl-3-methylimidazolium iodide (0.60 M), 38.1 mg of I<sub>2</sub> (0.03 M), 338.0 mg of 4-tert-butyl pyridine (0.50 M), 40.12 mg of lithium iodide (0.06 M) and 59.1 mg of guanidinium thiocyanate (0.10 M) into 5 mL of anhydrous acetonitrile. The sealed DSSCs were used for the photocurrent-voltage test with an active area of 0.16 cm<sup>2</sup>. The symmetrical dummy cells used for EIS and Tafel-polarization measurement were assembled by two identical CEs, clipping the electrolyte similar to the one used for fabricating the DSSCs.

## **Materials Characterizations:**

X-ray diffraction (XRD) was performed on a Shimadzu XRD-6000 with CuK $\alpha$  radiation, X-ray tube voltage 40 kV and current 30 mA, respectively. Energy dispersive spectroscopy (EDS) of CZGS NPs on a silicon substrate was performed to analyze the elemental composition using a Hitachi SU-70 equipped with EDS detector. Transmission electron microscopy (TEM, JEOL, JEM-2100) were used to characterize the morphology and structure. X-ray photoelectron spectroscopy (XPS) was performed with a VG Scientific ESCLAB 220iXL X-ray photoelectron spectrometer. Raman spectra of CZGS nanocrystals were collected from a Dilor XY Labram spectrometer equipped with an Olympus BX40 confocal microscope under ambient conditions by using a ArHe green laser. The photocurrent-voltage tests of DSSCs were performed under AM 1.5 illumination ( $100 \text{ mWcm}^{-2}$ ) in ambient conditions on a 94023A Oriel sol3A solar simulator (Newport Oriel solar simulator newport stratford, inc.) with 450w xenon lamp as light source. The EIS experiments and Tafel-polarization curves were measured with dummy cells in the dark by using a Zahner electrochemical workstation (Zahner Co., Germany). The frequency range of EIS experiments was from 10 mHz to  $10^6$  Hz with an AC modulation signal of 10 mV and bias DC voltage of 0 V, in dark condition. The resultant impedance spectra were analyzed by means of the Zview software. Tafel-polarization measurements were carried out with a scan rate of  $50 \text{ mVs}^{-1}$ . Cyclic voltammetry was conducted in a three-electrode system in an acetonitrile solution of 0.1 mmol LiClO<sub>4</sub>, 10 mmol LiI and 1 mmol I<sub>2</sub> at a scan rate of  $50 \text{ mVs}^{-1}$ . Platinum nets electrode served as a CE, and the Ag/AgCl couple was used as a reference electrode.

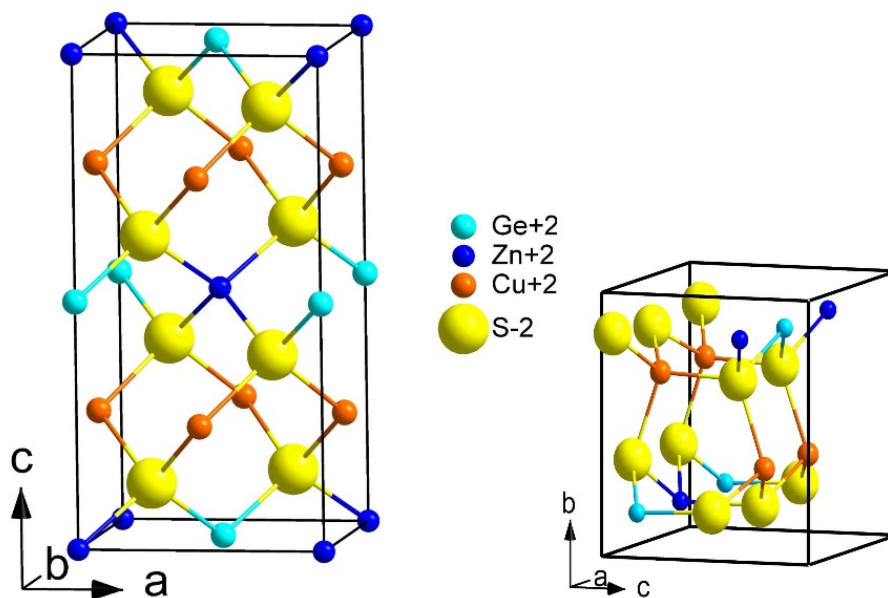


Fig. S1 Crystal structures of stannite (left) and wurtzstannite (right)  $\text{Cu}_2\text{ZnGeS}_4$ .

### Crystal structure

Molecular Formula	$\text{Cu}_2\text{ZnGeS}_4$	$\text{Cu}_2\text{ZnGeS}_4$
Crystal Structure	wurtzstannite	stannite
Space Group	$\text{Pmn}2_1$	$\text{I-}42\text{m}$
Crystal Parameter	$a=7.504 \text{ \AA};$ $b=6.474 \text{ \AA};$ $c=6.185 \text{ \AA};$	$a=b=5.270 \text{ \AA};$ $c=10.540 \text{ \AA}$

### Atomic Coordinates of wurtzstannite CZGS

Atom	Ox.	Wyck.	S.O.F.	x/a	y/b	z/c
Cu	+1	4b	1	0.75265	0.67580	0.17839
Zn	+2	2a	1	0	0.84203	0.66721
Ge	+4	2a	1	0	0.17054	0.17025

S	-2	2a	1	0	0.84538	0.05324
S	-2	2a	1	0	0.18374	0.53136
S	-2	4b	1	0.73909	0.65920	0.54749

#### Atomic Coordinates of stannite CZGS

Atom	Ox.	Wyck.	S.O.F.	x/a	y/b	z/c
Cu	+1	4d	1	0	0.5	0.25
Zn	+2	2a	1	0	0	0
Ge	+4	2b	1	0	0	0.5
S	-2	8i	1	0.256	0.256	0.119

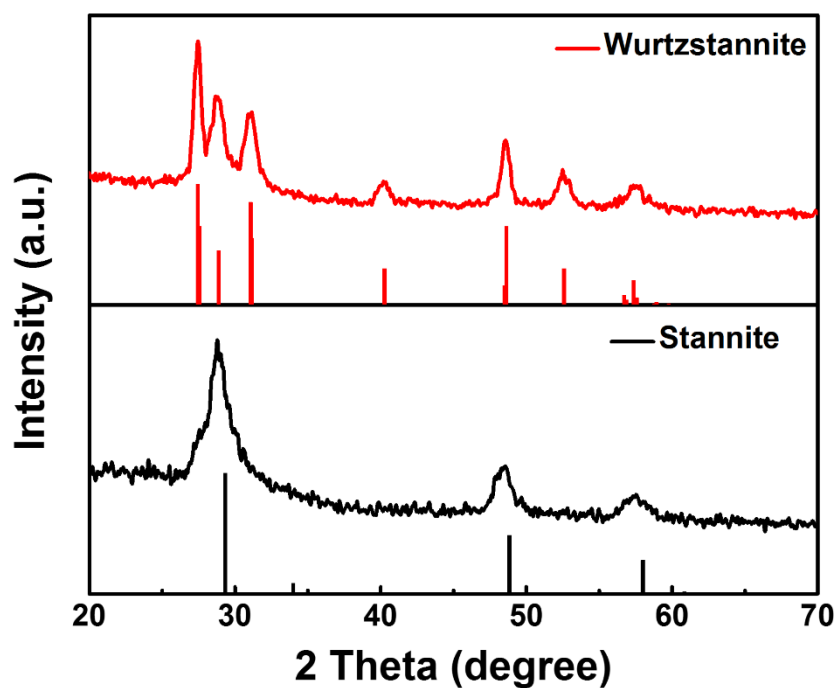


Fig. S2 XRD spectrum of the as-synthesized wurtzstannite-phase  $\text{Cu}_2\text{ZnGeS}_4$  nanocrystals.

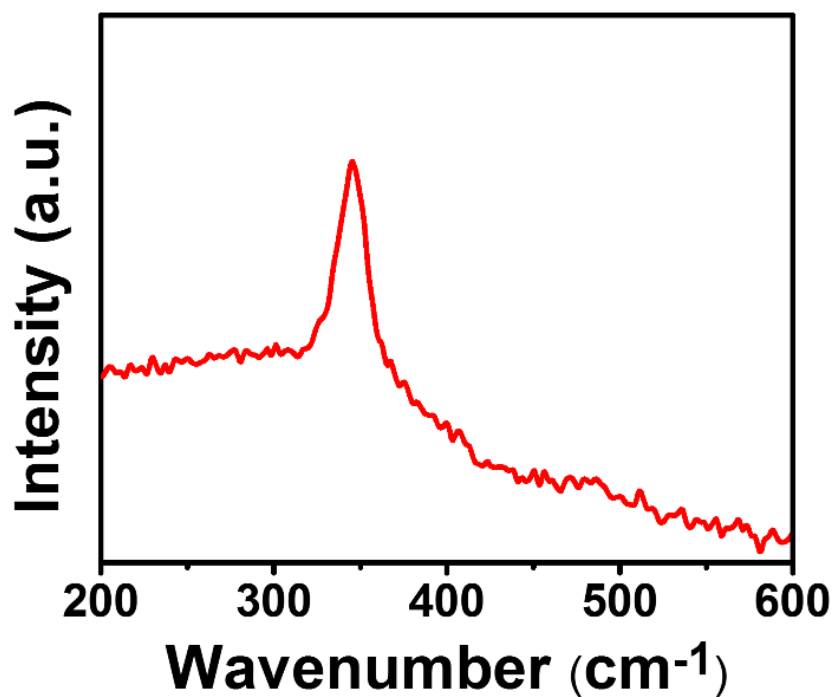


Fig. S3 Raman spectrum of the synthesized CZGS NCs.

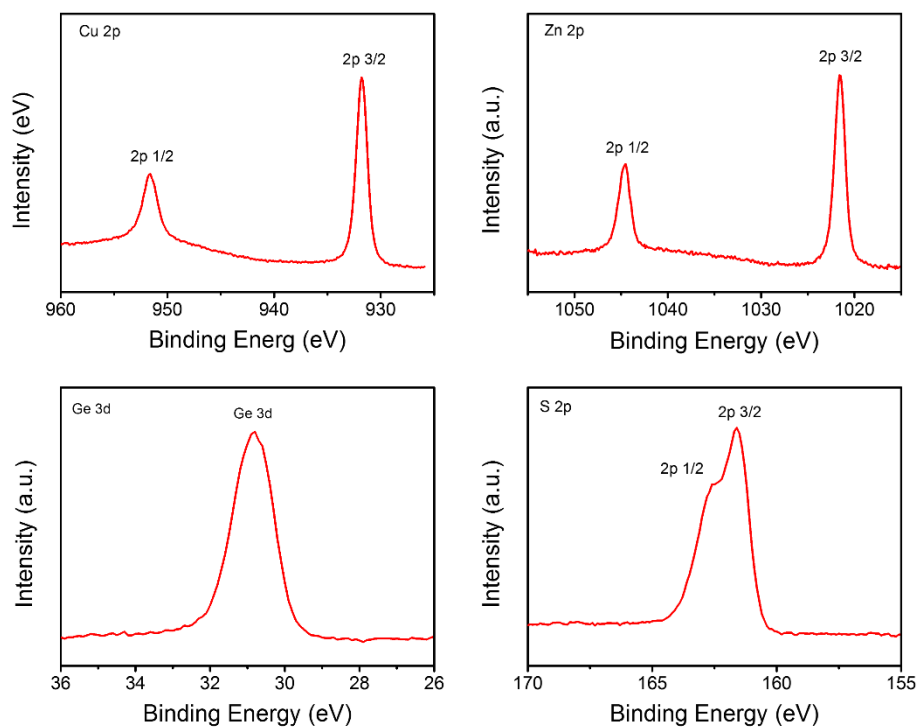


Fig. S4 XPS spectra of the as-obtained CZGS nanocrystals. The strong peaks of Cu 2p<sub>3/2</sub> and Cu 2p<sub>1/2</sub> located at 931.82 and 951.64 eV with a peak splitting of 19.82 eV (Fig. S2a) are well-consistent with

the reported values for  $\text{Cu}^+$ . No satellite peak of  $\text{Cu}^{2+}$  at about 942 eV for  $\text{Cu}_3\text{GeS}_4$  is observed in the present XPS spectrum. Hence, it is well proved that there is no existence of  $\text{Cu}_3\text{GeS}_4$  phase. The Zn 2p peaks located at 1021.77 and 1044.83 eV show a peak separation of 23.06 eV (Fig. S4-b), consistent with the standard splitting of 23.07 eV, suggesting  $\text{Zn}^{2+}$ . In the spectrum of Ge 3d (Fig. S4-c), it is observed that the peak locate at 30.81 eV corresponding to Ge 3d, indicating of  $\text{Ge}^{4+}$ . The binding energy of S 2p peak in the spectrum (Fig. S4-d) is 161.57 eV, which is in good agreement with the literature values for  $\text{S}^{2-}$ .

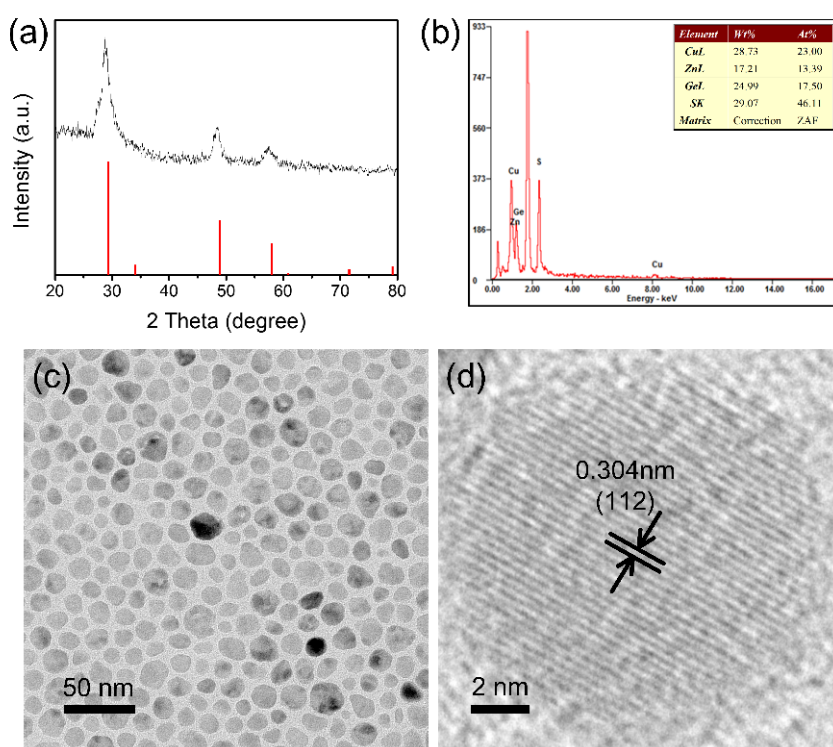


Fig. S5 (a) XRD and (b) EDS spectrum, (c) TEM image and (d) HRTEM image of the stannite-type CZGS NCs.



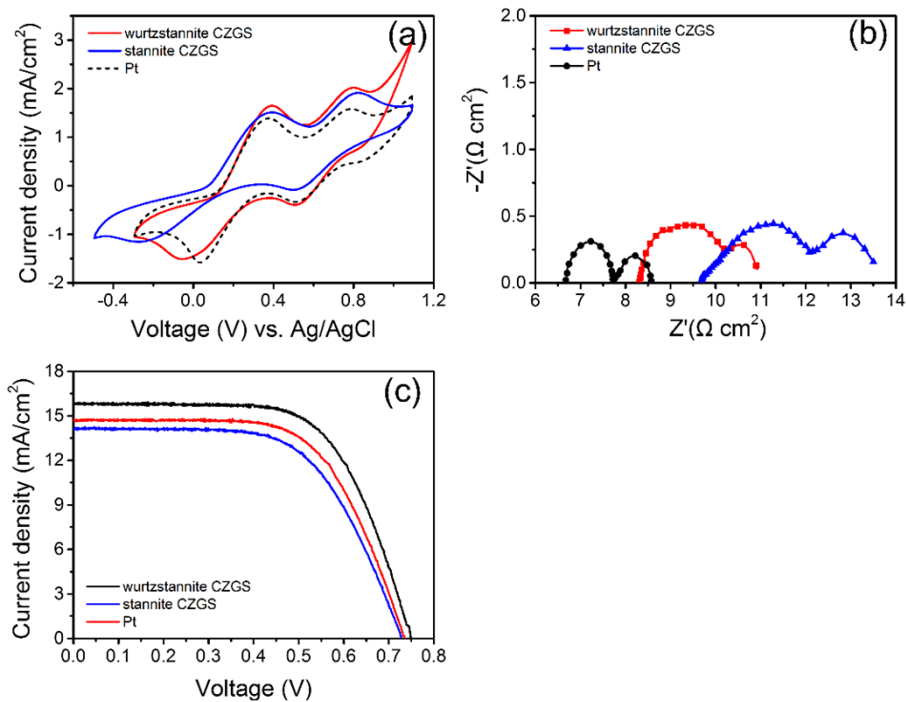


Fig. S6 (a) The cyclic voltammograms of the wurtzstannite-type CZGS, stannite-type CZGS and pyrolytic Pt CEs. (b) The EIS and (c) J-V characteristics of DSSCs with different CEs, measured at AM1.5G illumination ( $100 \text{ mW cm}^{-2}$ ).

Table S1. Photovoltaic performances of DSSCs with different CEs.

CE	$V_{oc}$ mV	$J_{sc}$ $\text{mA cm}^{-2}$	FF	PCE %
WZ-CZGS	736	14.72	0.63	6.85
SN-CZGS	729	14.15	0.60	6.15

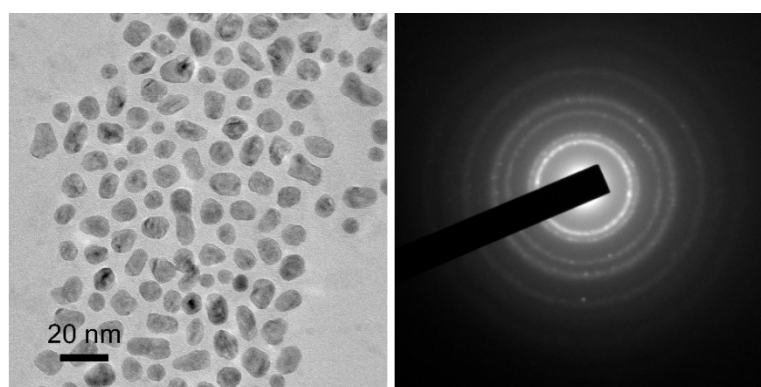


Fig. S7 TEM image (a) and SAED pattern of the as-synthesized  $\text{Pt}_3\text{Co}_1$  nanoparticles.

Table S2. Inductively coupled plasma atomic emission spectroscopy (ICP-AES) of the CZGS-PtCo sample.

element	Pt2144	Co2286
	%	%
1#	11.25	4.371
2#	11.40	4.376
3#	11.49	4.380
4#	11.42	4.372
<b>average</b>	<b>11.39</b>	<b>4.375</b>
SD (standard deviation)	0.10	0.004
%RSD (relative standard deviation)	0.9073	0.3077

Table S3. Fitted electrochemical parameters from EIS with symmetrical cells.

CE	CPE-T $\mu\text{F cm}^{-2}$	CPE-P	Ws-R	Ws-T	Ws-P
CZGS	19.54	0.52	0.79	0.39	0.49
Pt	28.94	0.76	0.85	0.58	0.47
PtCo	43.67	0.73	0.65	0.41	0.53
PtCo-CZGS	55.38	0.84	0.52	0.52	0.61

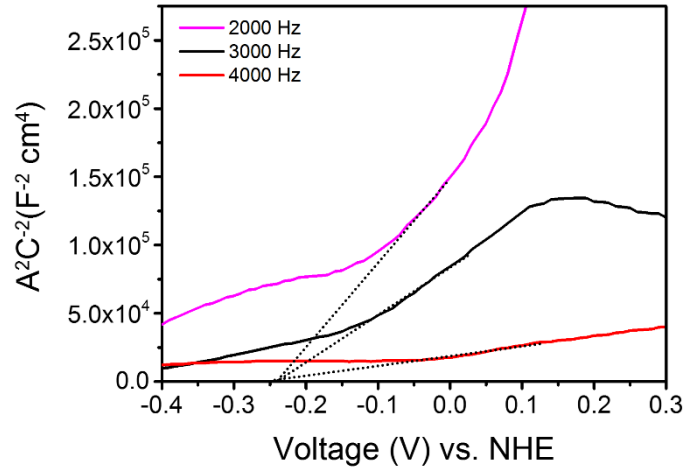


Fig. S8 Mott-Schottky relationship of CZGS electrode obtained for selected frequencies (2000 Hz to 4000 Hz) and determined by means of the method independent of frequency.

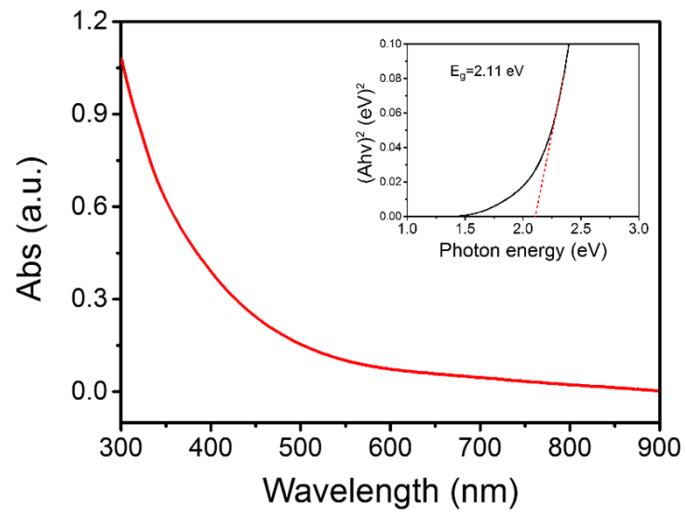


Fig. S9 UV-Vis spectra of the wurtzstannite phase CZGS nanocrystals.

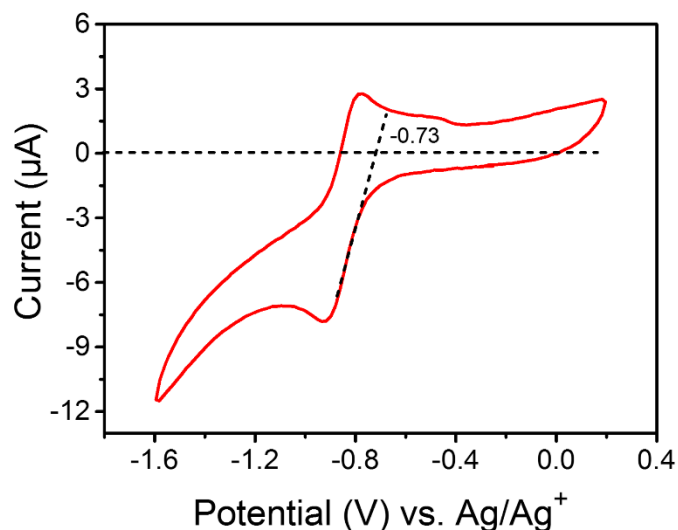


Fig. S10 Cyclic voltammograms of WZ-CZGS NCs using a  $\text{Ag}/\text{Ag}^+$  reference electrode.

The cyclic voltammograms (CVs) were recorded on a Zahner IM6 electrochemical workstation, using 3 mm glassy carbon as the working electrode, a Pt plate as the counter electrode, and  $\text{Ag}/\text{Ag}^+$  (Ag wires with 0.01 M  $\text{AgNO}_3$  in acetonitrile) as the reference electrode; 0.1 M tetrabutylammonium hexafluorophosphate (TBAPF6) dissolved in acetonitrile was employed as the supporting electrolyte. A typical CV curve for a wurtzite-type CZGS NCs thin film, deposited on a glassy carbon working electrode, is presented in Fig. S10.  $E_{\text{red}}$  appears at  $-0.73$  V relative to the  $\text{Ag}/\text{Ag}^+$  reference electrode. The conduction band minimum of the CZGS NCs was thereby determined to be  $-3.98$  eV from the vacuum level, and the valence band maximum was then estimated to be  $-6.09$  eV according to the 2.11 eV optical band gap. The result is agreement with the dynamic EIS analysis.

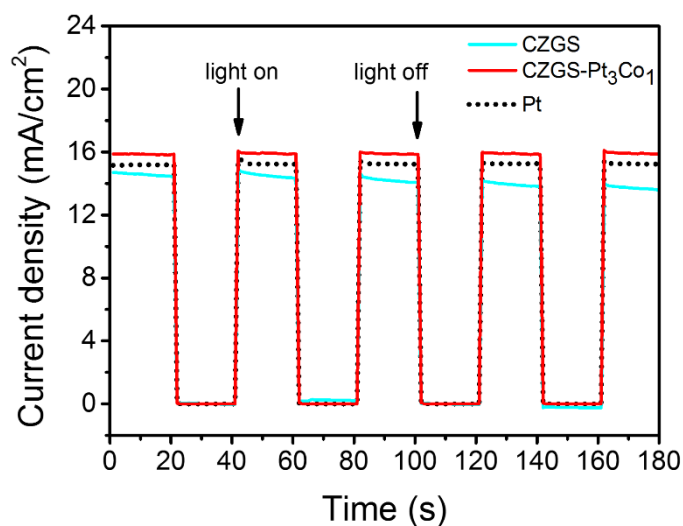


Fig. S11 Start-stop switches of the DSSCs with CZGS, CZGS-PtCo CE and Pt CE. The on-off plots are achieved by alternately irradiating ( $100 \text{ mW cm}^{-2}$ ) and darkening ( $0 \text{ mW cm}^{-2}$ ) the DSSC devices at 0.45 V, whereas the photocurrent stabilities are carried out under a sustained irradiation of  $100 \text{ mW cm}^{-2}$ .

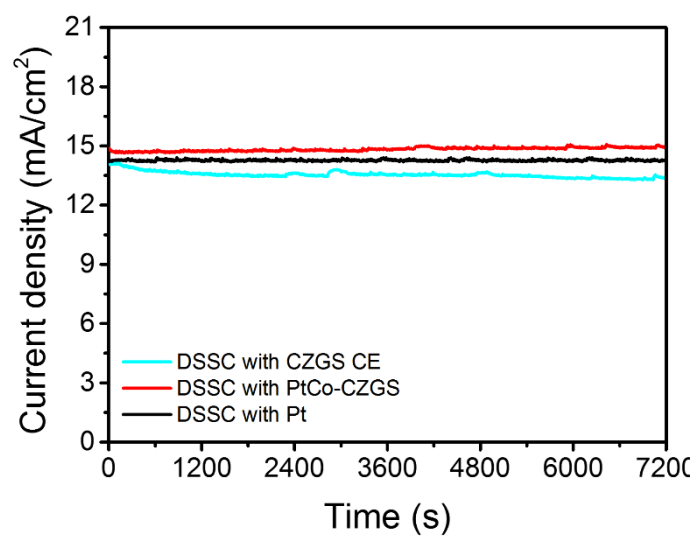


Fig. S12 Photocurrent stabilities of the DSSCs with CZGS, CZGS-PtCo and Pt CE under a sustained irradiation of 100 mW cm<sup>-2</sup>.

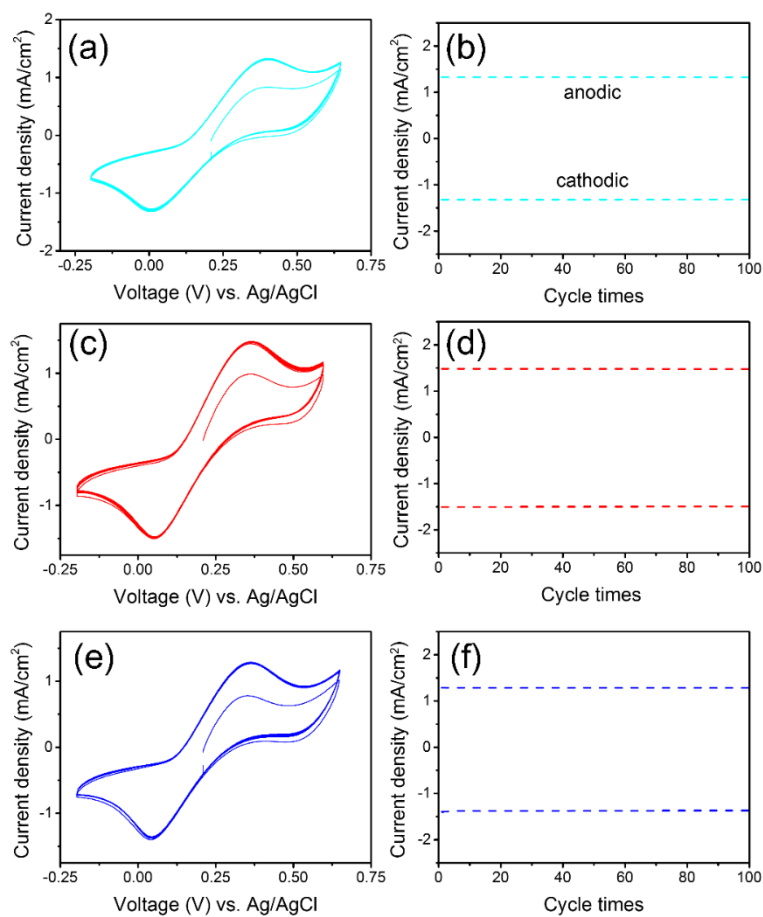


Fig. S13 100 consecutive CVs and the anodic and cathodic peak current densities versus cycle times of the CZGS based CE with the scan rate of 50 mV s<sup>-1</sup> in 10 mM LiI, 1 mM I<sub>2</sub>, and 0.1 M LiClO<sub>4</sub> acetonitrile: (a,b) CZGS, (c,d) CZGS-PtCo and (e,f) Pt.

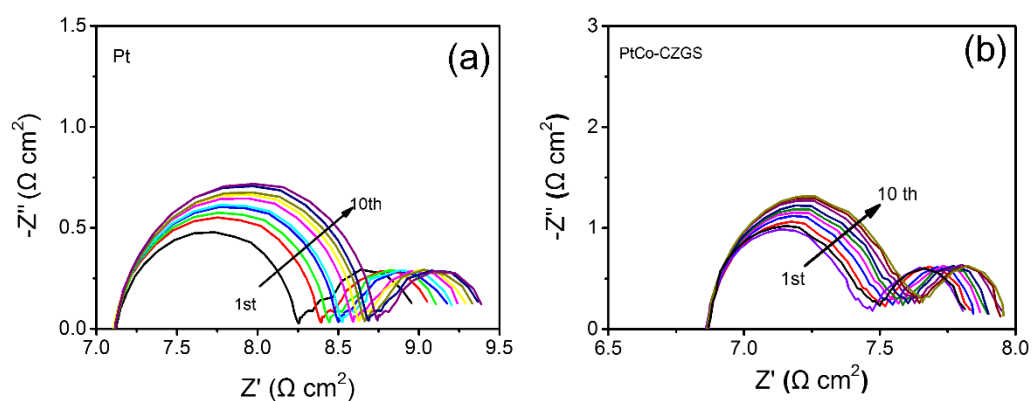


Fig. R14 Nyquist plots of EIS for the symmetrical cells with Pt (a) and PtCo-CZGS (b) CEs. The cell was first subjected to CV scanning from 0 to 1 V and then from -1 to 0 V with a scan rate of 100 mV s<sup>-1</sup>, followed by 60 s relaxation at 0 V, and then EIS measurement at 0 V from 0.1 Hz to 1M Hz was performed. This sequential electrochemical test was repeated 10 times.

#### Reference

1. X. L. Yu, A. Shavel, X. Q. An, Z. S. Luo, M. Ibanez and A. Cabot, *J. Am. Chem. Soc.*, 2014, **136**, 9236-9239.
2. S. E. Habas, P. D. Yang and T. Mokari, *J. Am. Chem. Soc.*, 2008, **130**, 3294-3295.
3. Y. S. Yu, W. W. Yang, X. L. Sun, W. L. Zhu, X. Z. Li, D. J. Sellmyer and S. H. Sun, *Nano Lett.*, 2014, **14**, 2778-2782.